Elastic scattering of electrons by GeH_4 in the low- and intermediate-energy range

M.-T. Lee
Departamento de Química, Universidade Federal de São Carlos, 13565-905 São Carlos, São Paulo, Brazil

L. M. Brescansin
Instituto de Física, Universidade Estadual de Campinas, 13083-970 Campinas, São Paulo, Brazil

L. E. Machado
Departamento de Física, Universidade Federal de São Carlos, 13565-905 São Carlos, São Paulo, Brazil

(Received 4 June 1998)

Elastic differential, integral, and momentum-transfer cross sections are reported for electron scattering by GeH_4 at impact energies ranging from 0.2 to 100 eV. The Schwinger iterative variational method in the fixed-nuclei, static-exchange plus correlation-polarization approximation is used to calculate the scattering amplitudes. Large-angular-momentum contributions from the correlation-polarization potential to the scattering amplitude are taken into account via a closed formula for higher incident energies. We have observed a T_2 shape resonance in the ICSs and MTCSs at around 3.0 eV and we have predicted a Ramsauer-Townsend minimum at around 0.6 eV. Our calculated cross sections are compared with recent experimental data and other theoretical results. [S1050-2947(99)00102-X]

PACS number(s): 34.80.Bm

I. INTRODUCTION

In spite of its importance in the chemistry of low-temperature plasmas and in the physics of semiconductors [1], electron scattering by germane has so far received little attention, either experimentally or theoretically. On the other hand, the demand on reliable cross sections for electron scattering by polyatomic targets has grown continuously and such quantities have been needed for several practical applications. In contrast with other group-IV tetrahydrides (such as CH_4 and SiH_4), which have been subjects of extensive theoretical and/or experimental investigations in the field of electron-molecule collisions, only a few experimental studies on e^--GeH_4 elastic scattering have been reported in the literature. Dillon *et al.* [2] have determined elastic and vibrationally inelastic cross sections for e^--GeH_4 collisions for incident energies between 1 and 100 eV. To our knowledge, this is the only report on differential cross sections for this molecule. Recently, absolute total cross sections for e^--GeH_4 collisions have been measured using the linear electron transmission technique by Karwasz [3] at intermediate (between 75 and 4000 eV) energies and by Mozejko *et al.* [4] for impact energies ranging from 0.75 to 250 eV.

From a theoretical point of view, the studies on e^--GeH_4 elastic scattering have been equally scarce. Differential cross sections (DCSs), momentum-transfer cross sections (MTCSs), and integral cross sections (ICSs) for elastic e^--GeH_4 collisions have been calculated in recent years at a few different levels of approximation. Winstead *et al.* [5] reported elastic DCSs, calculated within the static-exchange (SE) approximation, from 5 to 20 eV using the Schwinger multichannel method. The Schwinger multichannel method using pseudopotentials, also at the SE level, was applied by Bettega *et al.* [6] to study elastic scattering of electrons by GeH_4 molecules. Beyond the SE level, model potentials have been used and correlation-polarization contributions to the interaction potential have been taken into account via an approximated local function. Using a spherical effective potential in a static-exchange-polarization (SEP) approximation, Jain *et al.* [7] studied e^--GeH_4 scattering in the energy range 1–100 eV. Total (elastic plus inelastic) cross sections for e^--GeH_4 collisions have been calculated by Baluja *et al.* [8] using a spherical complex optical potential.

In this work we report calculated DCSs, ICSs, and MTCSs for elastic scattering of electrons by GeH_4 for incident energies ranging from 0.2 to 100 eV. Our scattering amplitudes are calculated using the Schwinger variational iterative method (SVIM) [9], a tool capable of providing highly converged estimates of the partial-wave T-matrix elements and scattering wave functions. In recent years the SVIM has been widely used for calculations on elastic electron-molecule scattering [10–15] and molecular photoionization [16–19]. It provides continuum wave functions that are shown to converge to the exact solutions for a given projectile-target interaction potential [20]. Fully *ab initio* calculations using the SVIM have led to reliable cross sections and other related parameters over a wide range of incident energies, in a number of previous applications. However, except for a study on photoionization of methane [16], the use of the SVIM was until recently limited to linear and planar polyatomic molecular targets. In addition, those applications of the method have been restricted to the SE level of approximation. On the other hand, accurate descriptions of the electron-molecule collision dynamics at the low-energy range usually require treatments beyond the SE level, namely, an appropriate balance of electrostatic, exchange, and correlation-polarization potentials [21]. Yet the inclusion of polarization effects has shown to produce elastic cross sections qualitatively different from the SE value at low energies [22]. We have recently extended our SVIM codes in order to treat nonplanar molecules with symmetry reducible to C_{2v}. Also, in this extended version a local correlation-

polarization contribution to the electron-molecule interaction potential has been included, following a prescription recommended by Padial and Norcross [23]. This extended version of our codes was applied to study elastic electron scattering by CH_4 [22] and SiH_4 [24], the results of both applications being very encouraging. Due to computational limitations, however, the range of incident energies E_0 in our previous studies has been rather restricted, namely, $E_0 \leqslant 50$ eV, the limitation being imposed on the number of partial waves employed in the single-center expansions of the SVIM. To our knowledge, the present work constitutes the first study on e^--GeH_4 collisions beyond the SE level, with the interaction potential being derived from fully molecular wave functions. Also, in order to consider incident energies $E_0 \geqslant 60$ eV, higher-order angular-momentum phase shifts are included in the calculation of the scattering amplitudes via a closed formula.

The organization of this paper is the following. In Sec. II the theory of the SVIM is briefly described and some details of the calculations are given. Our calculated cross sections and a discussion are presented in Sec. III. We conclude briefly in Sec. IV.

II. THEORY AND CALCULATION

The Schrödinger equation for the continuum scattering orbitals can be written (in atomic units) as

$$[-\nabla^2 + U(\vec{r}) - k^2]\Psi_{\vec{k}}(\vec{r}) = 0, \tag{1}$$

where $U(\vec{r}) = 2V(\vec{r})$ and $V(\vec{r})$ is the interaction potential between the target and the scattering electron. Equation (1) can be converted into an equivalent Lippmann-Schwinger equation

$$\Psi_{\vec{k}}^{(\pm)} = \Phi_{\vec{k}} + G_0^{(\pm)} U \Psi_{\vec{k}}^{(\pm)}, \tag{2}$$

with $G_0^{(\pm)}$ being the free-particle Green's operator with outgoing-wave ($G_0^{(+)}$) or incoming-wave ($G_0^{(-)}$) boundary conditions. In order to take advantage of the symmetry of the target, the scattering wave functions can be partial-wave expanded as

$$\Psi_{\vec{k}}^{(\pm)}(\vec{r}) = \left[\frac{2}{\pi}\right]^{1/2} \frac{1}{k} \sum_{p,\mu,l,h} i^l \Psi_{k,lh}^{(\pm)p\mu}(\vec{r}) X_{lh}^{p\mu}(\hat{k}), \tag{3}$$

where $X_{lh}^{p\mu}(\hat{r})$ are generalized spherical harmonics, related to the usual spherical harmonics Y_{lm} by

$$X_{lh}^{p\mu}(\hat{r}) = \sum_m b_{lhm}^{p\mu} Y_{lm}(\hat{r}). \tag{4}$$

Here p is an irreducible representation (IR) of the molecular point group, μ is a component of this representation, and h distinguishes between different bases of the same IR corresponding to the same value of l. The coefficients $b_{lhm}^{p\mu}$ satisfy important orthogonality conditions and are tabulated for the C_{2v} and O_h groups by Burke *et al.* [25]. The Schwinger variational expression for the T matrix can be written in the bilinear form as

$$T_{\vec{k},\vec{k}_0}^{(\pm)} = \langle \Phi_{\vec{k}}^{(\mp)} | U | \tilde{\Psi}_{\vec{k}_0}^{(\pm)} \rangle + \langle \tilde{\Psi}_{\vec{k}}^{(\mp)} | U | \Phi_{\vec{k}_0}^{(\pm)} \rangle - \langle \tilde{\Psi}_{\vec{k}}^{(\mp)} | U - U G_0^{(\pm)} U | \tilde{\Psi}_{\vec{k}_0}^{(\pm)} \rangle, \tag{5}$$

with $\tilde{\Psi}_{\vec{k}}^{(\pm)}$ denoting trial scattering wave functions. Using partial-wave expansions similar to Eq. (3) for both $\tilde{\Psi}_{\vec{k}}^{(\pm)}$ and the free-particle wave vector $\Phi_{\vec{k}}^{(\pm)}$, a partial-wave on-shell T matrix (diagonal in both p and μ) is obtained:

$$T_{k,lh;l'h'}^{(\pm)p\mu} = \langle \Phi_{k,l'h'}^{(\mp)p\mu} | U | \tilde{\Psi}_{k,lh}^{(\pm)p\mu} \rangle + \langle \tilde{\Psi}_{k,l'h'}^{(\mp)p\mu} | U | \Phi_{k,lh}^{(\pm)p\mu} \rangle - \langle \tilde{\Psi}_{k,l'h'}^{(\mp)p\mu} | U - U G_0^{(\pm)} U | \tilde{\Psi}_{k,lh}^{(\pm)p\mu} \rangle, \tag{6}$$

where $k = |\vec{k}_0| = |\vec{k}|$ for the elastic process.

The initial scattering wave functions can be expanded in a set R_0 of L^2 basis functions $\alpha_i(\vec{r}) = \langle \vec{r} | \alpha_i \rangle$:

$$\tilde{\Psi}_{k,lh}^{(\pm)p\mu}(\vec{r}) = \sum_{i=1}^{N} a_{i,lh}^{(\pm)p\mu}(k) \alpha_i(\vec{r}). \tag{7}$$

Using Eqs. (6) and (7), variational $T_{k,lh;l'h'}^{(\pm)p\mu}$ matrix elements can be derived as

$$T_{k,lh;l'h'}^{(\pm)p\mu} = \sum_{i,j=1}^{N} \langle \Phi_{k,l'h'}^{(\mp)p\mu} | U | \alpha_i \rangle [D^{(\pm)^{-1}}]_{ij} \langle \alpha_j | U | \Phi_{k,lh}^{(\pm)p\mu} \rangle, \tag{8}$$

where

$$D_{ij}^{(\pm)} = \langle \alpha_i | U - U G_0^{(\pm)} U | \alpha_j \rangle \tag{9}$$

and the corresponding approximate scattering solution with outgoing-wave boundary condition becomes

$$\Psi_{k,lh}^{(+)p\mu^{(S_0)}}(\vec{r}) = \Phi_{k,lh}^{p\mu}(\vec{r}) + \sum_{i,j=1}^{M} \langle \vec{r} | G_0^{(+)} U | \alpha_i \rangle \times [D^{(+)^{-1}}]_{ij} \langle \alpha_j | U | \Phi_{k,lh}^{p\mu} \rangle. \tag{10}$$

Converged outgoing solutions of Eq. (2) can be obtained via an iterative procedure. The method consists in augmenting the basis set R_0 by the set

$$S_0 = \{\Psi_{k,l_1h_1}^{(+)p\mu^{(S_0)}}(\vec{r}), \Psi_{k,l_2h_2}^{(+)p\mu^{(S_0)}}(\vec{r}), \ldots, \Psi_{k,l_ch_c}^{(+)p\mu^{(S_0)}}(\vec{r})\}, \tag{11}$$

where l_c is the maximum value of l for which the expansion of the scattering solution (3) is truncated. A new set of partial wave scattering solutions can now be obtained from

$$\Psi_{k,lh}^{(+)p\mu^{(S_1)}}(\vec{r}) = \Phi_{k,lh}^{p\mu}(\vec{r}) + \sum_{i,j=1}^{M} \langle \vec{r} | G^{(+)} U | \eta_i^{(S_0)} \rangle \times [D^{(+)^{-1}}]_{ij} \langle \eta_j^{(S_0)} | U | \Phi_{k,lh}^{p\mu} \rangle, \tag{12}$$

where $\eta_i^{(S_0)}(\vec{r})$ is any function in the set $R_1 = R_0 \cup S_0$ and M is the number of functions in R_1. This iterative procedure continues until a converged $\Psi_{k,lh}^{(+)p\mu^{(S_n)}}$ is achieved. These

TABLE I. Cartesian Gaussian functions used in the SCF calculations. Cartesian Gaussian basis functions are defined as $\phi^{\alpha,\prime,m,n,\mathbf{A}}(\mathbf{r})=N(x-\mathbf{A}_x)^{\prime}(y-\mathbf{A}_y)^m(z-\mathbf{A}_z)^n\exp(-\alpha|\mathbf{r}-\mathbf{A}|^2)$, with N a normalization constant.

	s		*p*		*d*	
Atom	Expt.	Coefficient	Expt.	Coefficient	Expt.	Coefficient
Ge	357500	0.000839	2345.000	0.0225140	74.8400	0.030390
	53670.00	0.006264	554.2000	0.1833500	21.230000	0.173190
	12300.00	0.032036	177.3000	0.860030	7.297000	0.440090
	3512.000	0.127510	66.13000	0.343060	2.549000	0.565320
	1161.000	0.391650	26.90000	0.506520	0.816500	1.000000
	428.0000	0.545280	11.26000	0.261410	0.684000	1.000000
	428.0000	0.181600	11.26000	0.067246	0.228000	1.000000
	170.0000	0.622480	6.116000	0.372380	0.076000	1.000000
	72.06000	0.248720	2.819000	0.617630		
	26.69000	1.000000	1.211000	1.000000		
	11.50000	1.000000	0.356800	1.000000		
	3.742000	1.000000	0.162100	1.000000		
	1.499000	1.000000	0.060840	1.000000		
	0.229200	1.000000	0.023000	1.000000		
	0.086750	1.000000		0.00000		
	0.023000	1.000000				
H	33.6444	1.000000	1.00000	1.000000		
	5.05796	1.000000	0.50000	1.000000		
	1.14680	1.000000	0.10000	1.000000		
	0.321144	1.000000				
	0.101309	1.000000				

converged scattering wave functions correspond, in fact, to exact solutions of the truncated Lippmann-Schwinger equation with the potential U [20].

In an actual calculation we compute the converged partial wave K-matrix elements $K^{p\mu^{(S_n)}}_{k,lh;l'h'}$. These K-matrix elements can be obtained by replacing $D^{(+)}$ by its principal value $D^{(P)}$ in Eq. (8). Hence the corresponding partial-wave T-matrix elements can be calculated from

$$T^{p\mu^{(S_n)}}_{k,lh,l'h'}=-\left[\frac{2}{\pi}\right]\sum_{l'',h''}\left[1-iK^{(S_n)}\right]^{p\mu}_{k,lh;l''h''}K^{p\mu^{(S_n)}}_{k,l''h'';l'h'}. \tag{13}$$

By usual transformations, these matrix elements can be expressed in the laboratory frame (LF). The LF scattering amplitude $f(\hat{k}'\hat{k}'_0)$ is related to the T matrix by

$$f(\hat{k}',\hat{k}'_0)=-2\pi^2T, \tag{14}$$

where $\hat{k}'_0$ and $\hat{k}'$ are the directions of incident and scattered electron linear momenta, respectively. The differential cross section for elastic electron-molecule scattering is given by

$$\frac{d\sigma}{d\Omega}=\frac{1}{8\pi^2}\int d\alpha(\sin\beta)d\beta\,d\gamma|f(\hat{k}',\hat{k}'_0)|^2. \tag{15}$$

Here α,β,γ are the Euler angles that define the orientation of the principal axes of the molecule. Finally, after some angular-momentum algebra, the LF DCSs averaged over the molecular orientations can be written as

$$\frac{d\sigma}{d\Omega}=\sum_L A_L(k)P_L(\cos\theta), \tag{16}$$

where θ is the scattering angle. The coefficients $A_L(k)$ in Eq. (16) are given by the formula

$$\begin{aligned}A_L(k)=&\frac{1}{2}\frac{1}{2L+1}\sum_{\substack{p,\mu,l,h,l',h',m,m'\\ p_1,\mu_1,l_1,h_1,l'_1,h'_1,m_1,m'_1}}\\ &\times(-1)^{m'-m}\sqrt{(2l+1)(2l_1+1)}\\ &\times b^{p_1\mu_1}_{l'_1h'_1m'_1}b^{p_1\mu_1^*}_{l_1h_1m_1}b^{p\mu^*}_{l'h'm'}b^{p\mu}_{lhm}a^{p_1\mu_1^*}_{l_1h_1,l'_1h'_1}(k)a^{p\mu}_{lh,l'h'}(k)\\ &\times(l_10l0|L0)(l'_10l'0|L0)(l_1-m_1lm|L-M)\\ &\times(l'_1m'_1l'm'|LM),\end{aligned} \tag{17}$$

where $(j_1m_1j_2m_2|j_3m_3)$ are the usual Clebsch-Gordan coefficients and the auxiliary amplitudes $a^{p\mu}_{lh,l'h'}(k)$ are defined as

$$a^{p\mu}_{lh,l'h'}(k) = -\frac{\sqrt{\pi^3}}{k} i^{l'-l}\sqrt{2l'+1}\,T^{p\mu(S_n)}_{k,lh;l'h'}. \quad (18)$$

In our study U is an optical potential that includes both an exact static-exchange part and a model correlation-polarization (CP) contribution. Following the prescription of Padial and Norcross [23], this contribution is introduced in the potential through a parameter-free model that combines the target correlation calculated from the local electron-gas theory for short distances with the asymptotic form of the polarization potential, given (for T_d molecules) by

$$v_p(\vec{r}) = -\frac{1}{2}\frac{\alpha_0}{r^4}, \quad (19)$$

where α_0 is the spherical part of the molecular dipole polarizability. In our calculations the experimental value $\alpha_0 = 44.353a_0^3$ was taken [26]. For energies $E_0 \geqslant 60$ eV, an additional term that accounts for the contributions of angular momenta higher than l_c is included in the scattering amplitude calculation as

$$f(\hat{k}',\hat{k}'_0) = \sum_{l,h,l',h'}^{l_c,l'_c} f_{l,h,l',h'} + f^{(higher)}, \quad (20)$$

where

$$f^{(higher)} = \frac{1}{2ik}\sum_{l=l_c+1}^{l_{max}} (2l+1)(e^{2i\delta_l}-1)P_l(\cos\theta) \quad (21)$$

and δ_l is the partial-wave phase shift, given by a closed formula [27]

$$\tan\delta_l = -\frac{\pi k^2 \alpha_0}{(2l-1)(2l+1)(2l+3)}. \quad (22)$$

The self-consistent-field (SCF) wave function for the ground state was obtained using the contracted Gaussian basis set shown in Table I. At the equilibrium Ge-H bond distance ($R_{Ge-H} = 2.8857$ a.u.) this basis set gives a SCF energy of -2123.2697 a.u. In the present calculation the cutoff parameter used in the expansions of the target bound orbitals and the static-plus CP potential is $l_c = 18$. All possible values of $h \leqslant l$ are retained. With this cutoff, the normalization of all bound orbitals is better than 0.999. In SVIM calculations, we have limited the partial-wave expansions to $l_c = 18$ for energies $E_0 \geqslant 60$ eV, $l_c = 16$ for $20 \leqslant E_0 < 60$ eV, and $l_c = 12$ for lower energies. In addition, specifically for $E_0 = 60$ eV and $E_0 = 100$ eV, higher-angular-momentum phase shifts up to $l_{max} = 200$ were used in Eq. (21). In order to verify the convergence of our partial-wave expansions, cross sections for $E_0 = 60$ eV and $E_0 = 100$ eV were calculated considering the cutoff parameters $l_c = 16$ and $l_c = 18$. No significant differences have been noticed in the cross sections calculated with $l_c = 16$ and $l_c = 18$ for both energies, thus ensuring the convergence of our partial-wave expansions.

The discussion of the convergence in the iterative procedure is also interesting in itself. In the present calculations, it has been verified that the convergence of the eigenphase sums is better than 0.1% within six iterations for all scattering symmetries and for all energies considered herein.

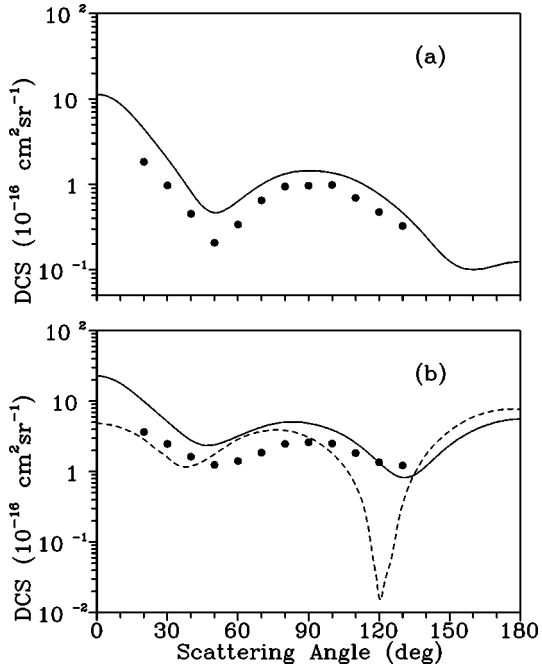

FIG. 1. DCSs for elastic e^--GeH_4 scattering at an impact energy of (a) 1 eV and (b) 2 eV. Solid line, present results; short-dashed line, spherical SEP results of Jain *et al.* [7]; full circles, experimental results of Dillon *et al.* [2].

III. RESULTS AND DISCUSSION

We have selected representative results on DCSs, mostly where experimental data and/or other calculations are available for comparison. The calculated DCSs for e^--GeH_4 scattering in the (1–100)-eV incident energy range are shown in Figs. 1–5, along with the experimental results of Dillon *et al.* [2] (see also Table II). Theoretical cross sections of Jain *et al.* [7], Winstead *et al.* [5], and Bettega *et al.* [6] are also included for comparison, whenever available. In general, there is good qualitative agreement between our calculated results and the measured data [2]. Quantitatively, the best agreement between our data and experiment is observed at energies from 5 to 10 eV. At lower energies, our theory overestimates significantly the DCSs. This discrepancy is somewhat expected and is attributed to the failure of the fixed-nuclei approximation when applied to electron-molecule scattering near resonances. Only calculations that explicitly account for nuclear vibrational motions can remove these discrepancies [28]. In the present case, as we will see below, there is a strong d-wave ($l = 2$) shape resonance in the T_2 scattering channel at incident energies near 3 eV. For incident energies $E_0 \geqslant 15$ eV, our theory overestimates the DCSs for intermediate and large scattering angles. The reason for this disagreement is the existence of absorption effects, not included in the present investigation. As known, at impact energies above excitation and ionization thresholds the flux of the scattered electrons is distributed over all open channels, consequently resulting in a reduction of the flux corresponding to the elastic scattering.

When compared with other calculations, the SE-level re-

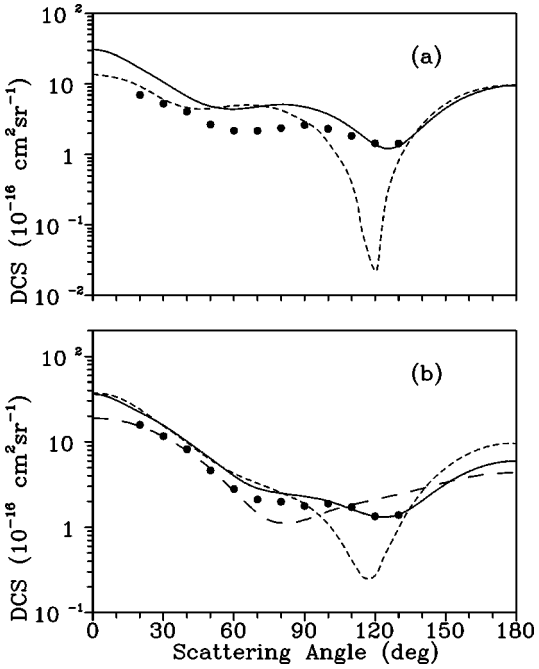

FIG. 2. Same as Fig. 1, but for (a) 3 eV and (b) 5 eV. Long-dashed line, SE results of Winstead *et al.* [5].

sults of Bettega *et al.* [6] agree quite well with our theoretical data wherever the comparison was possible, except at small scattering angles where their calculations cannot reproduce correctly the enhancement of DCSs in the forward direction. Although the calculations of Winstead *et al.* [5] and Bettega *et al.* [6] are on the same level of approximation, significant differences between their results can be observed at some energies. On the other hand, the calculated results of Jain *et al.* [7] using the spherical SEP potential show a deep minimum at around 120° for incident energies $E_0 < 10$ eV.

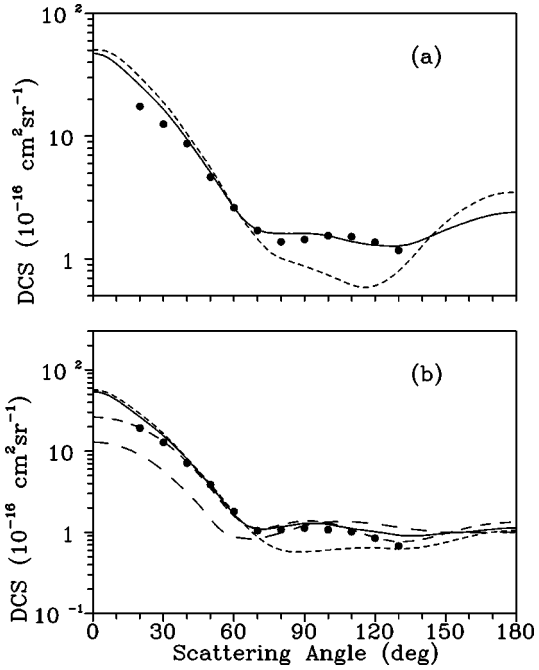

FIG. 3. Same as Fig. 2, but for (a) 7.5 eV and (b) 10 eV. Dashed line, pseudopotential SE results of Bettega *et al.* [6].

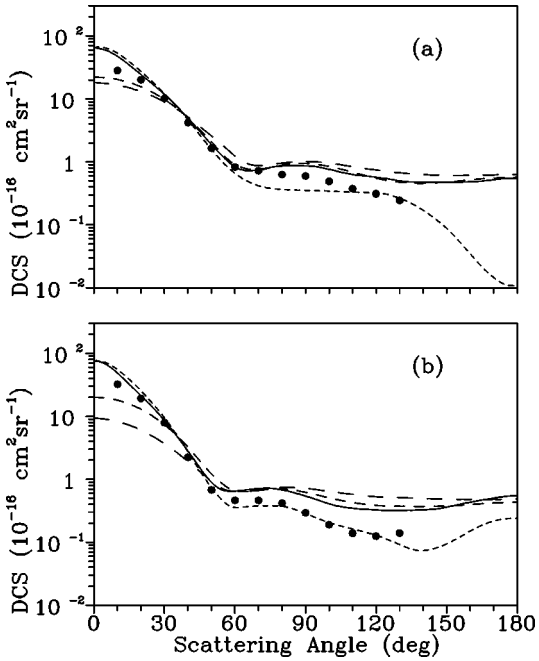

FIG. 4. Same as Fig. 3, but for (a) 15 eV and (b) 20 eV.

This well pronounced minimum results from the lack of non-spherical components of the interaction potential in their calculation. At higher energies, however, their results are on better agreement with the experimental data than ours. We have also calculated DCSs for incident energies below 1 eV, as shown in Fig. 6. Unfortunately, neither other theoretical nor experimental results are available for comparison in this energy range.

The present calculation does not account for relativistic effects. Nevertheless, the influence of these effects on the

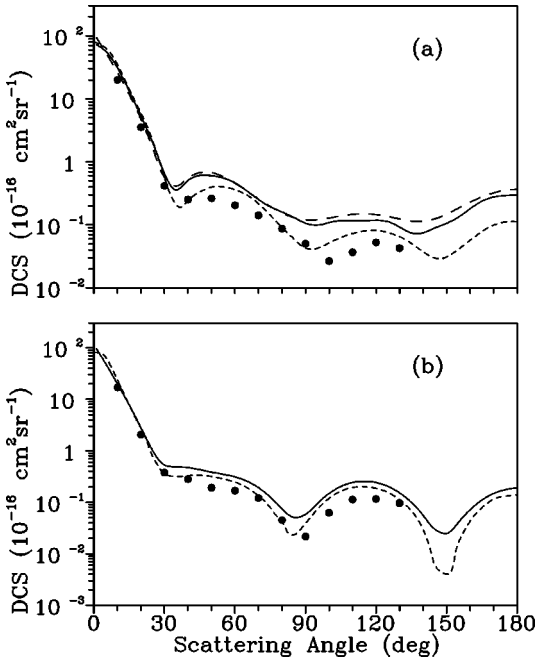

FIG. 5. Same as Fig. 1, but for (a) 60 eV and (b) 100 eV. Solid line, present results with $l_c = 16$; dashed line, present results with $l_c = 18$; short-dashed line, spherical SEP results of Jain *et al.* [7]; full circles, experimental results of Dillon *et al.* [2].

TABLE II. DCSs, ICSs, and MTCSs (in 10^{-16} cm^2) for elastic e^--GeH_4 scattering.

Angle	E_0 (eV)								
(deg)	1	2	3	5	7.5	10	20	60	100
0	11.37	22.81	30.80	36.20	47.49	54.15	76.72	72.46	96.60
10	8.69	17.82	25.37	30.60	38.87	42.74	48.49	31.13	19.84
20	4.45	9.92	16.72	22.17	26.00	26.30	21.16	5.33	2.80
30	2.00	5.11	10.63	15.57	16.57	15.46	8.53	0.650	0.528
40	0.821	2.79	6.68	10.11	9.46	8.01	2.80	0.507	0.473
50	0.464	2.40	4.82	6.39	5.06	3.74	0.890	0.604	0.385
60	0.635	3.18	4.41	3.99	2.63	1.67	0.647	0.464	0.311
70	0.994	4.29	4.76	2.85	1.73	1.10	0.711	0.252	0.192
80	1.33	5.03	5.10	2.50	1.61	1.17	0.680	0.160	0.748
90	1.44	4.86	4.73	2.30	1.61	1.28	0.542	0.106	0.058
100	1.36	3.92	3.72	2.03	1.54	1.25	0.408	0.109	0.148
110	1.11	2.57	2.40	1.63	1.39	1.11	0.347	0.16	0.242
120	0.768	1.34	1.39	1.34	1.30	1.02	0.325	0.118	0.242
130	0.465	0.822	1.32	1.41	1.28	0.925	0.320	0.092	0.152
140	0.243	1.20	2.43	2.05	1.43	0.914	0.326	0.075	0.056
150	0.126	2.36	4.52	3.19	1.72	0.971	0.361	0.106	0.025
160	0.100	3.81	6.87	4.50	2.03	1.02	0.432	0.180	0.072
170	0.112	5.04	8.77	5.56	2.29	1.09	0.501	0.277	0.148
180	0.124	5.56	9.54	5.96	2.40	1.14	0.552	0.297	0.188
ICS	14.25	45.92	63.31	60.01	54.30	47.57	30.65	12.10	8.86
MTCS	9.84	36.40	46.93	33.95	24.06	17.54	7.16	2.21	2.05

calculated cross sections can be estimated through the comparison with the calculated DCS of Bettega *et al.* [6]. Relativistic effects are somehow included in the pseudopotentials used in their studies. The good agreement between the DCS of these two calculations, except at small scattering angles (where the polarization effects are more important), is an indication that the influence of the relativistic effects is small for a molecule as heavy as germane. Indeed, a theoretical study by Lam [29] on the relativistic effects in elastic electron scattering by krypton, an isoelectronic system of germane, has also led to the same conclusion.

In Figs. 7 and 8 we compare our calculated ICSs and MTCSs, respectively, with the calculated results of Jain *et al.* [7], Winstead *et al.* [5], and Bettega *et al.* [6], as well as with the measured elastic ICSs and MTCSs of Dillon *et al.* [2] and with the total cross sections (TCSs) of Mozejko *et al.* [4] and Karwasz [3]. The corresponding data below 1 eV are shown in the insets of the figures. Our results show a minimum at around 0.6 eV and a strong resonance feature around 3 eV. In order to identify the physical origin of these structures, we have carried out an eigenphase analysis, which is

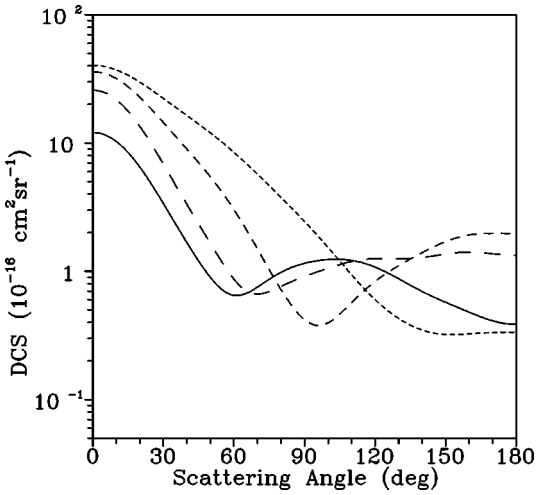

FIG. 6. Present DCSs below 1 eV. Solid line, 0.8 eV; long-dashed line, 0.6 eV; dashed line, 0.4 eV; short-dashed line, 0.2 eV.

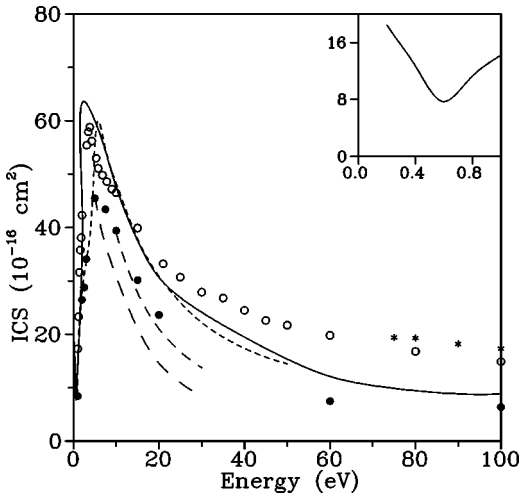

FIG. 7. ICSs for elastic e^--GeH_4 scattering. Solid line, present results; short-dashed line, spherical SEP results of Jain *et al.* [7]; dashed line, pseudopotential SE results of Bettega *et al.* [6]; long-dashed line, SE results of Winstead *et al.* [5]; full circles, experimental results of Dillon *et al.* [2]; open circles, absolute total cross sections from Mozejko *et al.* [4]; asterisks, absolute total cross sections from Karwasz [3]. Inset: present elastic ICSs below 1 eV.

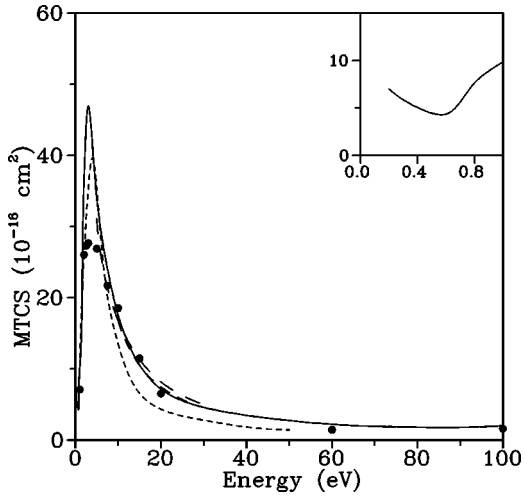

FIG. 8. MTCSs for elastic e^--GeH_4 scattering. The symbols are the same as in Fig. 7. Inset: present MTCSs below 1 eV.

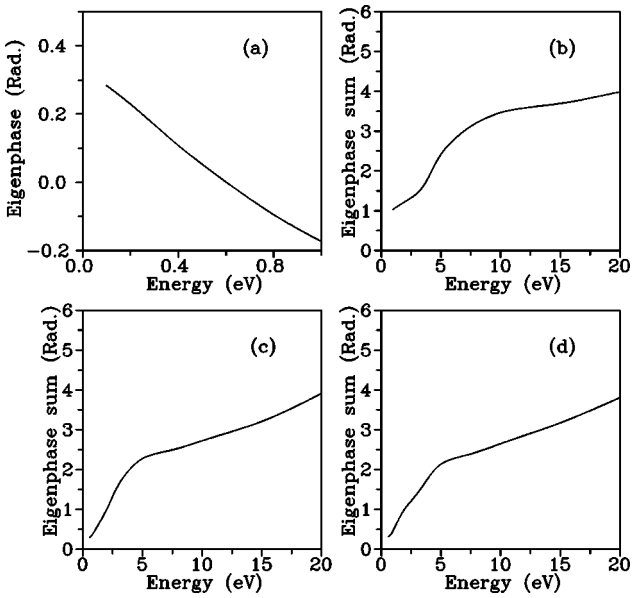

FIG. 9. (a) Eigenphase for the $l=0$ (S-wave) component in the (0.1–1)-eV range; (b), (c), and (d), eigenphase sums for the A_1, B_1, and B_2 components of the T_2 scattering symmetry, respectively, in the (1.0–20)-eV range.

shown in Fig. 9. The analysis of Fig. 9(a), which shows the eigenphase for $l=0$ (S wave), indicates that the minimum at around 0.6 eV is actually a Ramsauer-Townsend (RT) minimum. Also the eigenphase sums for the C_{2v}-reduced components (A_1, B_1, and B_2) of the T_2 scattering channel seen in Figs. 9(b)–9(d) show a shape resonance around 3 eV in this channel. The calculated position of this resonance is in good agreement with that observed in the measured ICSs, MTCSs, and TCSs. In addition, our calculated ICSs and MTCSs agree qualitatively with the measured data of Dillon *et al.*, [2] although they lie systematically above them. In general, the agreement in MTCSs is better than in the ICSs. Also, our ICSs are in very good agreement with the experimental TCSs of Mozejko *et al.* [4] for energies $E_0 \leqslant 20$ eV. Comparing with other theoretical results, the ICSs and MTCSs of Jain *et al.* [7] agree quite well with our data except at around the resonance region. As expected, the SE ICSs of Winstead *et al.* [5] and Bettega *et al.* [6] lie systematically below our data. However, very good agreement is seen in the comparison of their MTCSs and ours.

IV. CONCLUSION

In summary, we have reported the results of DCSs, ICSs, and MTCSs for e^--GeH_4 scattering over a wide range of incident energies. In general, our calculated results are in good agreement with experimental data reported in the literature. We have observed a T_2 shape resonance in the ICSs at around 3.0 eV. The position of this resonance is in accordance with experimental findings. In addition, our model was also able to predict a RT minimum in the ICSs and MTCSs at around 0.6 eV.

ACKNOWLEDGMENTS

This research was partially supported by the Conselho Nacional de Desenvolvimento Científico e Tecnológico (CNPq), FINEP-PADCT, CAPES-PADCT, and FAPESP.

[1] M. Stutzman, R. A. Street, C. C. Tsai, J. B. Boyce, and S. E. Ready, J. Appl. Phys. **94**, 568 (1989).
[2] M. A. Dillon, L. Boesten, H. Tanaka, M. Kimura, and H. Sato, J. Phys. B **26**, 3147 (1993).
[3] G. P. Karwasz, J. Phys. B **28**, 1301 (1995).
[4] P. Mozejko, G. Karperski, and C. Szmytkoski, J. Phys. B **29**, L571 (1996).
[5] C. Winstead, P. G. Hipes, M. A. P. Lima, and V. McKoy, J. Chem. Phys. **94**, 5455 (1991).
[6] M. H. F. Bettega, A. P. P. Natalense, M. A. P. Lima, and L. G. Ferreira, J. Chem. Phys. **103**, 10 566 (1995).
[7] A. Jain, K. L. Baluja, V. Di Martino, and F. A. Gianturco, Chem. Phys. Lett. **183**, 34 (1991).
[8] K. L. Baluja, A. Jain, V. Di Martino, and F. Gianturco, Europhys. Lett. **17**, 139 (1992).
[9] R. R. Lucchese, G. Raseev, and V. McKoy, Phys. Rev. A **25**, 2572 (1982).
[10] M.-T. Lee, L. M. Brescansin, M. A. P. Lima, L. E. Machado, and E. P. Leal, J. Phys. B **23**, 4331 (1990).
[11] L. M. Brescansin, M. A. P. Lima, L. E. Machado, and M.-T. Lee, Braz. J. Phys. **22**, 221 (1992).
[12] L. E. Machado, M.-T. Lee, L. M. Brescansin, M. A. P. Lima, and V. McKoy, J. Phys. B **28**, 467 (1995).
[13] L. E. Machado, E. P. Leal, M.-T. Lee, and L. M. Brescansin, J. Mol. Struct.: THEOCHEM **335**, 37 (1995).
[14] L. M. Brescansin, L. E. Machado, and M.-T. Lee, Phys. Rev. A **57**, 3504 (1998).
[15] M.-T. Lee, S. E. Michelin, T. Kroin, and L. E. Machado, J. Phys. B **31**, 1781 (1998).
[16] M. Braunstein, V. McKoy, L. E. Machado, L. M. Brescansin, and M. A. P. Lima, J. Chem. Phys. **89**, 2998 (1988).
[17] L. E. Machado, L. M. Brescansin, M. A. P. Lima, M. Braunstein, and V. McKoy, J. Chem. Phys. **92**, 2362 (1990).

[18] R. R. Lucchese and V. McKoy, Phys. Rev. A **28**, 1382 (1993).
[19] L. M. Brescansin, M.-T. Lee, L. E. Machado, M. A. P. Lima, and V. Mckoy, Braz. J. Phys. **27**, 468 (1997).
[20] R. R. Lucchese, D. K. Watson, and V. McKoy, Phys. Rev. A **22**, 421 (1980).
[21] B. I. Schneider, T. N. Rescigno, B. H. Lengsfield III, and C. W. McCurdy, Phys. Rev. Lett. **66**, 2728 (1991).
[22] L. E. Machado, M.-T. Lee, and L. M. Brescansin, Braz. J. Phys. **28**, 111 (1998).
[23] N. T. Padial and D. W. Norcross, Phys. Rev. A **29**, 1742 (1984).
[24] M.-T. Lee, L. E. Machado, and L. M. Brescansin, J. Mol. Struct.: THEOCHEM (to be published).
[25] P. G. Burke, N. Chandra, and G. N. Thompson, J. Phys. B **5**, 2212 (1972).
[26] T. M. Miller, *Chemistry and Physics* (CRC, Boca Raton, FL, 1984).
[27] Y. Jiang, J. Sung, and L. Wan, Phys. Rev. A **52**, 398 (1995).
[28] W. Sun, M. A. Morrison, W. A. Isaacs, W. K. Trail, D. Alle, R. J. Gulley, M. J. Brennan, and S. J. Buckman, Phys. Rev. A **52**, 1229 (1995).
[29] L. T. Sin Fai Lam, J. Phys. B **15**, 119 (1982).